

## AN ADVANCED MODEL FOR DOPANT DIFFUSION IN HEAVILY IMPLANTED POLYCRYSTALLINE SILICON THIN FILMS

Reçu le 13/01/2007 – Accepté le 09/10/2007

### Résumé

Ce travail est dédié à l'étude de la diffusion accélérée et transitoire (TED) du bore dans des films minces de silicium polycristallin. Cette diffusion est considérée comme un problème majeur pour le développement des dispositifs MOS à grille P<sup>+</sup> de polysilicium; pour de futures technologies en polysilicium. La grille fortement dopée, P<sup>+</sup>, est réalisée par implantation ionique suivie d'un recuit thermique d'activation. Dans ces conditions, le dopant bore diffuse de façon accélérée et anormale pouvant être de quelques mille de fois à quelques centaines de fois plus vite qu'à l'équilibre thermodynamique. En même temps, le dépassement de la solubilité solide dû au très fort dopage ainsi que les dommages créés par l'implantation ionique, entraînent l'apparition de divers phénomènes complexes tels que ségrégation, formation d'amas ou clusters, et piégeage du dopant. En tenant compte de ces phénomènes, nous proposons un modèle théorique uni-dimensionnel de deux-jet en diffusion adapté à la structure granulaire du polysilicium et aux effets des fortes concentrations. Ce modèle tient compte de la formation de clusters dans les grains ainsi que dans les joints de grains. D'ailleurs, la croissance des grains et l'augmentation de la barrière de potentiel aux joints de grains ont été combinées avec les coefficients de diffusion et le processus thermique basé sur les concepts thermodynamiques. L'ajustement des profils simulés avec les profils SIMS expérimentaux, pour des températures de recuit relativement basses (700, 750 et 800°C) et des durées comprises entre 1 et 30 minutes, permettra d'étudier la diffusion transitoire et accélérée du bore, ainsi que la compréhension de l'effet de la croissance des grains sur la redistribution du bore durant le recuit thermique.

**Mots clés:** modélisation, bore, diffusion, croissance du grain, joint de grains, polysilicium

### Abstract

This work is dedicated to the study of the transient enhanced diffusion (TED) of boron in polycrystalline-silicon thin films. This phenomenon is a major problem for the development of P<sup>+</sup> polysilicon gate metal-oxide-semiconductor (MOS) devices; for future polysilicon technologies. The highly doped, P<sup>+</sup>, gate is made by ion implantation followed by thermal post-implantation annealing. In these conditions, the boron atoms diffuse in a transient and enhanced way which can be some thousand times to some hundred times faster than in equilibrium. At the same time, the solubility limit excess due to the very strong doping level and ion-implantation damages, lead to various complex phenomena such as dopant trapping, segregation, and clustering. Taken all these phenomena into account, we propose a theoretical one-dimensional two-stream diffusion model adapted to the granular structure of polycrystalline-silicon and to the effects of the strong-concentrations. This model includes dopant clustering in grains as well as in grain boundaries. Moreover, growth of grains and energy barrier height are coupled with the dopant diffusion coefficients and the process temperature based on thermodynamic concepts. The adjustment of the simulated profiles with the experimental SIMS profiles, for short treatment times ranging between 1 and 30 minutes at different temperatures (700, 750 and 800°C), will allow the study of the boron transient enhanced diffusion; as well as the understanding of the grains-growth effect on boron diffusion during annealing.

**Keywords:** modeling, boron, diffusion, grain-growth, grain-boundaries, polysilicon.

S. ABADLI  
F. MANSOUR  
Département d'Electronique  
Faculté des Sciences de  
l'Ingénieur  
Université Mentouri  
Constantine - Algérie

### ملخص

إن هذا العمل مخصص لدراسة ظاهرة الانتشار السريع والانتقالي لذرات البور في رقائق السليسيوم متعدد البلورات. هذا الانتشار يعتبر بمثابة عائق حقيقي أمام تطوير المركبات الميكرو الإلكترونية ذات الشبكة P<sup>+</sup> من السليسيوم متعدد البلورات. لغرض استعمالات مستقبلية. هذه الشبكة الجد مطعمة P<sup>+</sup>. يتم إنجازها بطريقة الغرس الأيوني متبوعة بمعالجة حرارية لتنظيم تموقع الذرات و تنشيطها كهربائياً. في هذه الشروط، تنتشر ذرات التطعيم (البور) بطريقة سريعة و غير عادية حيث يمكن أن تكون آلاف أو مئات المرات أسرع من حالة الانتشار في حالة التوازن الترموديناميكي. في نفس الوقت، إجتياز قيمة الذوبان الحدية الناتج عن التطعيم المرتفع و أضرار الغرس الأيوني، يبدان عدة ظواهر فيزيائية معقدة كالحصر، تفريق ذرات التطعيم و تشكيل تكدسات من ذرات التطعيم. أخذين بعين الاعتبار كل هذه الظواهر، نقترح في هذه الدراسة نموذجاً للانتشار المزدوج أحادي البعد مكيف للبنية الحبيبية للسليسيوم متعدد البلورات و إلى تأثيرات التراكيز العالية للذرات. هذا النموذج يأخذ بعين الاعتبار حالة تشكيل تكدسات داخل الحبيبات و في روابط الحبيبات أيضاً. بالمعنى، نمو الحبيبات و زيادة حاجز الكمون في روابط الحبيبات تم إدماجها مع ثوابت الانتشار و التأثيرات الحرارية المتعلقة بالظواهر الترموديناميكية. إن مطابقة منحنيات التمثيل بتلك المحصل عليها تجريبياً بطريقة التحليل الطيفي لكل الأيونات SIMS، من أجل درجات معالجة حرارية ضعيفة نسبياً (700 و 800°م) و أزمنة محصورة بين 1 و 30 دقيقة، يسمح بدراسة الانتشار السريع و الانتقالي لذرات البور و فهم تأثير نمو الحبيبات على إعادة توزيع البور خلال المعالجة الحرارية.

**الكلمات المفتاحية:** نموذج، انتشار، البور، نمو الحبيبات، روابط الحبيبات، سليسيوم متعدد البلورات

The ability to self-align the gate electrodes of MOS field-effect transistors (MOSFET's) reduces capacitance and improves circuits speed. In addition to improving circuits speed, the compatibility of polycrystalline-silicon thin films with subsequent thermal processing allows its efficient integration into advanced integrated-circuits and permits fabrication of new devices structures [1], [2]. The heavily doped polysilicon is currently the more used gates material. In consequence, p<sup>+</sup> doped polysilicon gate electrodes have been used instead of n<sup>+</sup> polysilicon ones for p channel MOSFETs to convert the buried-channel operations to surface-channel ones [3], which are scalable to deep submicrometer dimensions. However, boron penetration from p<sup>+</sup> polysilicon gate electrodes through such thin gate oxide layers and into the underlying silicon channel region has become a severe problem [4] because a high carrier activation in the polysilicon is simultaneously required to prevent the gate depletion effect, which degrades the drivability of devices. Ion implantation remains the most used technique of doping; it allows a good control of diffusion profiles. However, the implanted dopant is generally electrically inactive and the energetic ions create a large concentration of defects or damages that degrade the device characteristics [5], [6]. Thermal post-implantation annealing is essential to treat the samples of its defects and to allow the implanted ions to take positions where they will be electrically active and able to exchange charges with the silicon atoms.

During this process, the presence of high boron-silicon clusters in grains as well as in grain boundaries causes transient enhanced diffusion (TED) of the dopant atoms [6], [7]. This poses an additional problem for the manufacture of micro-electronics components and advanced integrated-circuits.

With high-concentration of impurities, solid solubility limit can be exceeded and the doping excess precipitates and forms inactive and immobile clusters [8], [9]. Moreover, dopant forms electrically inactive and immobile clusters even at concentrations far below the solubility limit under the supersaturation of self-interstitials [6], [10]. Furthermore, during thermal annealing, dopant complex redistribution in polycrystalline-silicon is strongly affected by the morphological structure of polysilicon; grain boundaries provide disordered regions down which dopant atoms can readily diffuse. An additional complexity is that the morphological structure of polysilicon changes during annealing; with grains growing in size. These phenomena make the simulation of the diffusion profiles of high-concentrations more and more complex and difficult. To the author's knowledge, there have been a little simulation studies that fully take all of these phenomena into account in the case of simulation of heavily implanted boron in polysilicon. As a result, our aim is to develop a fundamental understanding of the boron transfer mechanisms inside polysilicon and developing a model for the process. Another aim is to more finely understanding the role of the grain boundary and that of the grains growing in size in the TED during the thermal post-implantation annealing. This will make it possible to optimize the manufacturing process of very shallow junctions and thus, to propose solutions to overcome the established problems. We propose a theoretical one-dimensional two stream diffusion model adapted to the granular structure of polysilicon and to the effects of the strong-concentrations. This model consists of two coupled partial differential equations (PDE's) of diffusion. The first is associated to the diffusion in the grains; while the second is associated to the diffusion in the grain boundaries. These two equations are coupled by a term which represents the transfer and the opposite transfer between the grains and the grain boundaries; by associating effects related to the strong-concentrations and that of trapping and segregation.

## 1. EXPERIMENTAL DETAILS AND INITIAL CONDITIONS

### 1.1. Experiment

The studied samples consist of 335-nm-thickness layers of amorphous silicon obtained at 465°C by low pressure chemical vapor deposition (LPCVD); from disilane  $\text{Si}_2\text{H}_6$  under total pressure of 200 mTorr. The films are deposited on oxidized monocrystalline-silicon substrates (P-type, (111), 120 nm of thermal oxide  $\text{SiO}_2$ ). These films are then boron implanted with a dose of  $4 \times 10^{15}$  atoms/cm<sup>2</sup> at an energy of 15 keV. In order to avoid long redistributions, post-implantation annealings were carried out at a relatively low temperatures (700, 750 and 800°C) and short times ranging between 1 and 30 minutes. The experimental doping profiles have been obtained by secondary ion mass spectrometry (SIMS) with a CAMECA IMS4F measuring device [11]. It enables us to obtain impurity concentration profiles as a function of the sample depth. Figure 1 shows the total boron distribution profile in the deposited films before annealing (just after ion implantation). This experimental profile will be used as a reference during the first simulation step.

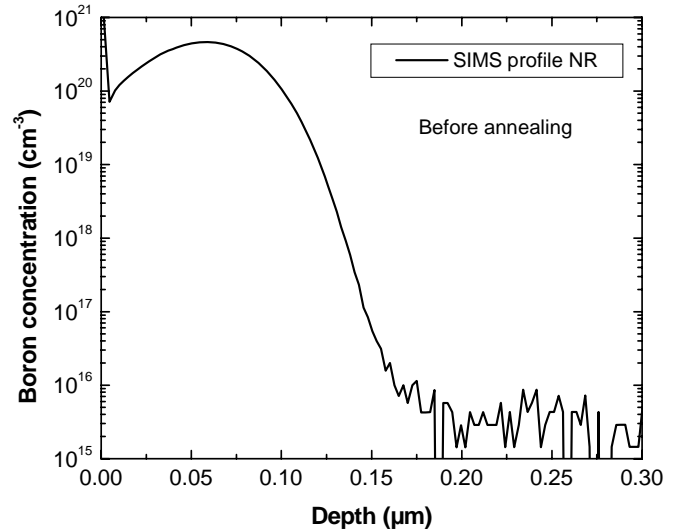


**Figure 1** : Boron distribution in the deposited film before annealing.

### 1.2. Initial conditions

The initial total boron distribution profile (before annealing), was easily simulated by the use of an analytical Gaussian expression identified by the three following parameters: the ion implantation dose,  $Q_d$ ; the projected range or peak concentration,  $R_p$ ; and the straggle or the standard deviation,  $\Delta R_p$ . This expression is given by the following form [12]:

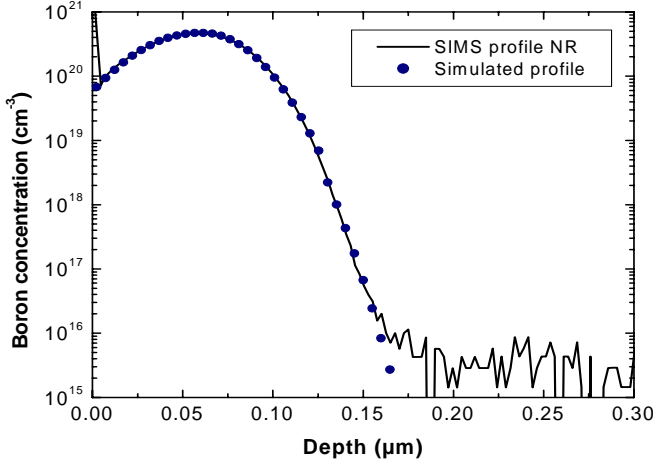
$$C(x) = \frac{Q_d}{\sqrt{2\pi} \Delta R_p} \exp\left(-\frac{(x - R_p)^2}{2\Delta R_p^2}\right) \quad (1)$$

Figure 2 shows the good superposition of SIMS profile before annealing and simulated profile. This first simulated profile will be used as initial condition during the next theoretical simulation steps. It will be introduced in the diffusion model as the initial total concentration ( $C_{tot}$ ).

For more knowledge, we used prolongation or extension of the Gaussian profile in its second part (after the peak concentration) because the Gaussian is not exactly symmetrical.

Starting from calculations carried out by using the expression given in Solmi *et al.* [13], for dopant solubility solid limit  $C_{sol}$  ( $C_{sol} = 9.25 \times 10^{22} \exp(-0.73/kT)$ ), we can inform that the implantation dose of  $4 \times 10^{15}$  atoms/cm<sup>2</sup> causes the solubility limit excess. In this case, the doping excess precipitates and forms inactive and immobile clusters [6], [9]. In the reality, the state of the dopant related to this parameter was not given in a clear and single way in the literature.

The ones suggests that dopant segregate to the grain boundaries when the dopant concentration exceeds its solubility limit [8], [14], while the others propose the possibility of clustering even at concentrations far below the solubility limit under the supersaturation of self-interstitials [6], [10] and [15].



**Figure 2** : Superposition of the simulated profiles with the experimental SIMS profile before annealing.

## 2. DIFFUSION MODEL

Recently, a lot of models had been proposed for the study and the simulation of the complex mechanisms of boron redistribution and activation in single-crystal or polycrystalline-silicon during the thermal post-implantation annealing [6], [11], and [16]. By using the ideas and the results of each model, we describe now a more detailed model adapted to the granular structure of polysilicon and to the effects of very strong-concentrations. The diffusion mechanism is controlled by two partial differential equations (PDE's), coupled by a term representing the dopant transfer between the grains and the grain boundaries. Hence, the total dopant concentration ( $C_{tot}$ ) will be divided between the grains ( $C_g$ ) and the grain boundaries ( $C_{gb}$ ).

The effects linked to the heavily-concentrations were combined with the dopant diffusion coefficients in the grains and the grain boundaries. As result, for a one-dimensional two-stream diffusion mechanism, this model is given by the next two coupled continuity equations for the two dopant concentrations  $C_g$  and  $C_{gb}$ :

$$\frac{\partial C_g}{\partial t} = \frac{\partial}{\partial x} \left( D_g^{eff} \frac{\partial C_g}{\partial x} \right) - k_t^{eff} \left( C_g - \frac{C_{gb}}{k_{seg}} \right) \quad (2)$$

$$\frac{\partial C_{gb}}{\partial t} = \frac{\partial}{\partial x} \left( D_{gb}^{eff} \frac{\partial C_{gb}}{\partial x} + \frac{D_g^{eff}}{L_g} C_{gb} \frac{\partial L_g}{\partial x} \right) + k_t^{eff} \left( C_g - \frac{C_{gb}}{k_{seg}} \right) \quad (3)$$

$C_g$  is the equilibrium dopant concentration in grains,  $C_{gb}$  is the equilibrium dopant concentration in grain boundaries,  $k_t^{eff}$  is the effective dopant transfer rate between grains and grain boundaries as a result of grain boundary movement,  $k_{seg}$  is the effective dopant segregation coefficient between the grains and the grain boundaries and  $L_g$  is the average grain size.

The two equations (2) and (3) have standard flux terms and are coupled together by the transfer of dopant atoms from the grains to the grain boundaries or vice versa [16], [17].

The driving force for diffusion being the gradient in the actual grain boundary concentration brings the  $L_g$  in the numerator in equation (3). In addition, the flux of dopant atoms in the grain boundary is proportional to the grain boundary volume and this explains the  $L_g$  in the denominator in equation (3) [16].

In consequence, the total dopant concentration in the studied layers is the sum of the two equilibrium concentrations  $C_{gb}$  and  $C_g$  ( $C_{total} = C_g + C_{gb}$ ). Therefore, it is necessary to deduce two theoretical profiles from the precedent simulated initial total diffusion profile (figure 2). This step was completed by using studies of Puchner *et al.* [16] and Sadovnikov [17].

The solubility limit  $C_{sol}$  is taken to calculate the active impurity concentration in grains  $C_g$  starting from the total impurity concentration  $C_{tot}$ . In effect, the reported expression of  $C_{sol}$  in Solmi *et al.* [13] is multiplied by a factor of 3 to have used values of  $C_{sol}$  for our polysilicon thin films.

$D_g^{eff}$  and  $D_{gb}^{eff}$  are respectively, the effective diffusion coefficients inside the grains and the grain boundaries. They take into account all the phenomena included in the model. These coefficients are identified by the next expressions:

$$D_g^{eff} = D_i \frac{1 + \beta(p/n_i)}{1 + \beta} \left( 1 + \frac{C_g}{\sqrt{C_g^2 + 4n_i^2}} \right) \left( 1 + m \left( \frac{C_g}{C_{sol}} \right)^{2m} \right)^{-1} \quad (4)$$

$$D_{gb}^{eff} = F_a D_i \frac{1 + \beta(p/n_i)}{1 + \beta} \left( 1 + \frac{C_{gb}}{\sqrt{C_{gb}^2 + 4n_i^2}} \right) \left( 1 - \exp\left(\frac{-E_b}{KT}\right) \right) \quad (5)$$

$$D_i = D_0 \exp\left(\frac{-E_a}{KT}\right) \quad (6)$$

where  $D_i$  is the intrinsic diffusion coefficient in single-crystal silicon,  $K$  is the Boltzmann constant,  $T$  is the annealing temperature in Kelvin,  $E_a$  is the activation energy,  $p$  is the holes concentration,  $n_i$  is the electron intrinsic concentration,  $C_{sol}$  is the solubility limit concentration for the dopant,  $\beta$  is a statistical factor for charged vacancies,  $m$  is the maximum number of boron and silicon atoms trapped in an interstitial cluster,  $F_a$  is a constant pre-exponential factor for the adjustment of the intrinsic diffusivity in the grain boundaries and  $E_b$  is the energy barrier height to the grain boundaries.

The intrinsic diffusivity in single-crystal silicon  $D_i$  varies exponentially with the temperature  $T$  and the activation energy  $E_a$  associated with the diffusion process. In our study, we took the very used value of  $E_a = 3.46$  eV [18], [19]; which is the default value for monocrystalline-silicon.  $D_0$  is the diffusivity pre-exponential factor ( $D_0 = 0.76$  cm<sup>2</sup>.s<sup>-1</sup>) [19].

The effective diffusion coefficient in the grains is greatly linked to the high-concentration effects (excess of  $C_{sol}$ ). It depends also on the charged vacancies-concentration in the interior grains; because of grains growth kinetics.  $\beta$  is the ratio of the diffusivity induced by the charged vacancies on the global diffusivity induced by the neutral vacancies;  $\beta = D_i^+ / D_i^0$  [11], [18].

In addition,  $D_g^{\text{eff}}$  depends of holes concentration  $p$  and intrinsic concentration  $n_i$ . Moreover, it depends of the doping solubility limit  $C_{\text{sol}}$ , as well as of the interstitial defects for small clusters size; with a maximum number  $m$  of self-interstitials and dopant atoms trapped in clusters [6], [16]. Concerning the effective diffusion coefficient in the grain boundaries  $D_{\text{gb}}^{\text{eff}}$ , it is well controlled by the trapping and the segregation to the grain boundaries.

These two effects are obviously related to the energy barrier height  $E_b$  to the grain boundaries [17].  $E_b$  depends even on the impurities concentration, the average size of the grains, and the traps density [20], [21].  $F_a$  is a constant factor for the adjustment of the intrinsic diffusivity within the grain boundaries (polycrystalline or amorphous silicon); since the diffusivity in single-crystal silicon is very different to that in polycrystalline silicon [18]. It represents the ratio  $D_{\text{poly}}/D_{\text{mono}}$  because the boron diffusion coefficient in polysilicon is much higher than the diffusion coefficient in monocrystalline silicon. This pre-exponential factor can be some hundreds to some thousand [11], [18].

The coupling between the two diffusion PDE's (2) and (3) is ensured by the term representing the effective dopants transfer from the grains to the grain boundaries and vice versa. The net effective transfer rate is given by [17], [22]:

$$k_t^{\text{eff}} = \frac{D_g}{L_g} \left( \frac{4}{L_g} + \frac{1}{2\sqrt{D_g t}} \right) + \frac{2\alpha}{L_g} \frac{\partial L_g}{\partial t} \quad (7)$$

The effective doping transfer rate between the grains and the grain boundaries depends mainly of the average grain size  $L_g$  and its growth during thermal annealing (morphological changes and crystallization).  $\alpha$  is a factor of adjustment [22]; in this work we take  $\alpha = 1$ . In real polycrystalline silicon, the crystallites have a distribution of sizes and irregular shapes. To simplify the study, we assume that polysilicon is composed of identical crystallites having a grain size of  $L_g$ . The grains are assumed to be squares growing from initial grain size  $L_{g0}$ . The grain-growth kinetic is proportional to the square root of time [17], [23]:

$$L_g(t) = \sqrt{L_{g0}^2 + 2\gamma t} \quad (8)$$

$L_g(t)$  represents the average grains size after time  $t$  and  $L_{g0}$  represents the initial average grains size; grains size just after deposition of polysilicon layer.  $\gamma$  is a parameter which depends on the grain boundary mobility and the grain boundary energy ( $\gamma = 4.6 \times 10^{-2} \exp(-1.36/KT) \mu\text{m}^2/\text{s}$ ) [23]. Its value depends on the local Fermi level. Concerning the dopant segregation coefficient  $k_{\text{seg}}$ , it can be described by using the results of Mandurah *et al.* [24] and Swaminathan *et al.* [25]. It is known by the next expression:

$$k_{\text{seg}} = 2 k_{\text{seg0}} \frac{e_{\text{gb}}}{L_g} \quad (9)$$

$k_{\text{seg0}}$  is the thermal equilibrium grain boundary segregation coefficient and  $e_{\text{gb}}$  is the average width of a grain boundary. Segregation coefficient is described by the expression analogous to one in Mandurah *et al.* [24] and to that in Sadovnikov [17] ( $k_{\text{seg0}} = k_0 \exp(0.456/KT)$ ).

Concerning the estimated values of  $E_b$ , they have been calculated by using the following relations [20], [21]:

- For total impurity concentration  $C_{\text{tot}}$  lower than a critical concentration  $C^*$  ( $C_{\text{tot}} < C^*$ ), the energy barrier  $E_b$  is calculated by using the equation (10).

$$E_b = \frac{q^2 L_g^2}{8\epsilon} C_{\text{tot}} \quad (10)$$

- For total impurity concentration  $C_{\text{tot}}$  higher than a critical concentration  $C^*$  ( $C_{\text{tot}} > C^*$ ), the energy barrier  $E_b$  is calculated by using the equations (11) and (12).

$$E_b \cong \frac{q^2 N_t^2}{8\epsilon C_{\text{tot}}} \quad \text{if} \quad E_F - E_b \gg KT \quad (11)$$

$$E_b \cong \frac{E_g}{2} + KT \ln \left( q \frac{N_t}{N_c} \sqrt{\frac{C_{\text{tot}}}{2\epsilon E_b}} \right) \quad (12)$$

where  $E_g$  is the band-gap energy,  $E_b$  is the barrier height,  $E_F$  is the Fermi level,  $N_c$  is the effective density of states relative to the conduction band,  $N_t$  is the density of the grain-boundaries traps and  $\epsilon$  is the dielectric permittivity of poly-Si.

### 3. RESULTS AND DISCUSSION

The simulated boron diffusion profiles were calculated by means of a realized program which makes the numerical resolution of the PDE's (2) and (3); while using a finite differences implicit method with specified boundary and initial conditions. The simulation well reproduces the experimental SIMS profiles leads to illustrate the significant role of the grains growing in size and that of the dopant trapping and segregation for the precise simulation of the diffusion profiles. The good adjustment is obtained while varying the following parameters:  $L_{g0}$ ,  $F_a$ ,  $m$ ,  $\beta$  and  $k_{\text{seg0}}$ .

Figures 3–8, show clearly the excellent adjustment of the simulated total profiles with SIMS profiles. These figures illustrate  $C_g$ ,  $C_{\text{gb}}$ , and  $C_{\text{total}}$  concentrations as a function of layers depth.

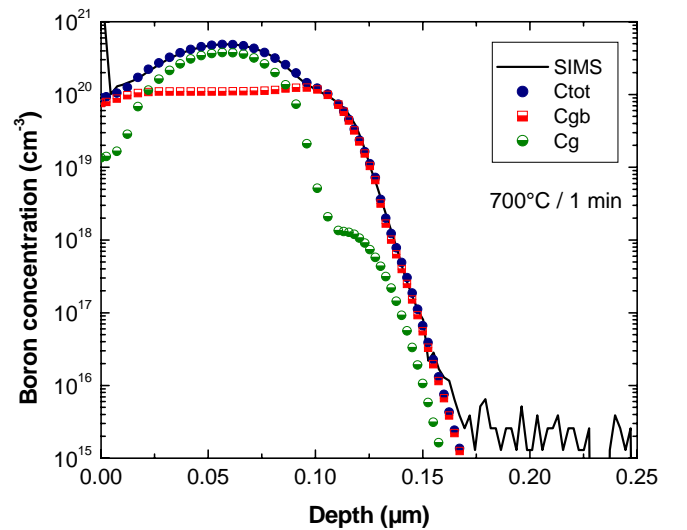


**Figure 3** : Superposition of the simulated profiles with the experimental SIMS profile after annealing at 700°C/1 min

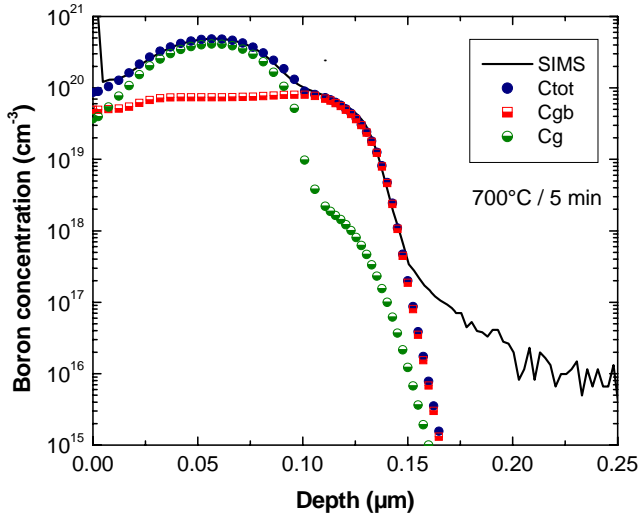


**Figure 4** : Superposition of the simulated profiles with the experimental SIMS profile after annealing at 700°C/5 min.

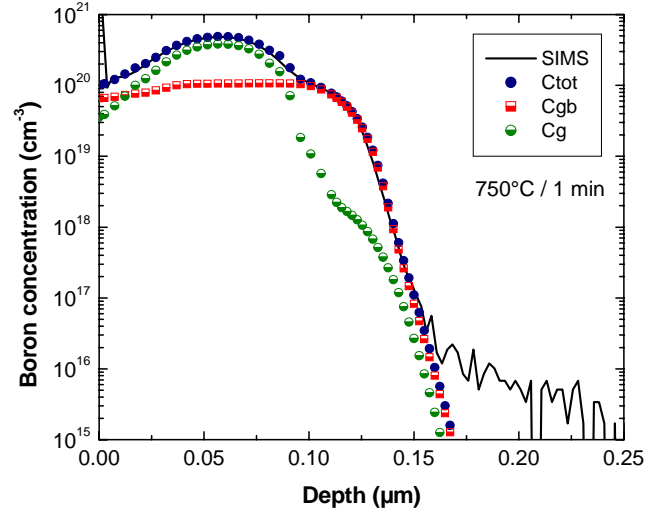


**Figure 4** : Superposition of the simulated profiles with the experimental SIMS profile after annealing at 750°C/1 min.

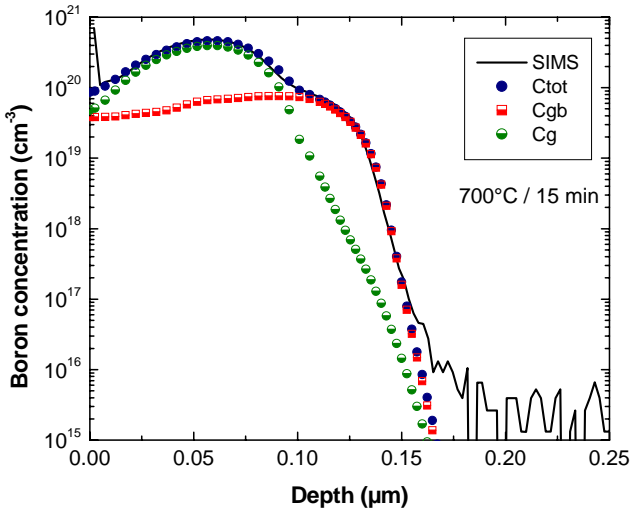


**Figure 5** : Superposition of the simulated profiles with the experimental SIMS profile after annealing at 700°C/15 min.

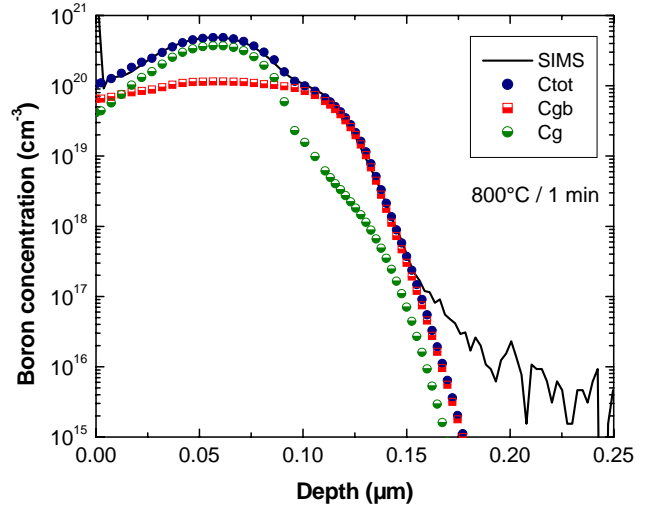


**Figure 8** : Superposition of the simulated profiles with the experimental SIMS profile after annealing at 800°C/1 min.

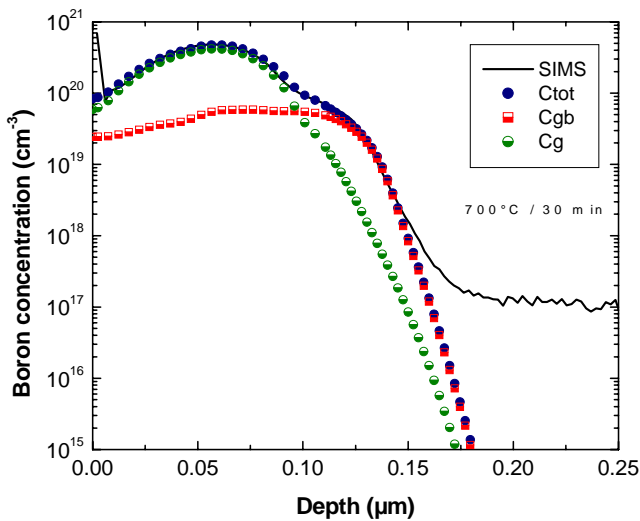


**Figure 6** : Superposition of the simulated profiles with the experimental SIMS profile after annealing at 700°C/30 min.

We notice good matching, particularly for the profiles shoulder that occurs for the boron solubility limit. This good adjustment indicates the validation of this model and confirms that the grains growing in size play a significant role for the precise determination of the diffusion profiles. We can tell that the boron diffusivity in the grains is not very different to that in the grain boundaries. This is justified by the significant reduction of the diffusion coefficient in the grain boundaries caused by the important trapping-segregation mechanism. In consequence, the effective diffusion coefficient in grain boundary depends much on  $E_b$ ,  $L_g$ , and thus on the density of trapping states. This density was found to be of the order of  $5 \times 10^{12} \text{ cm}^{-2}$ , while the grain boundary width  $e_{gb}$  is fixed at 13 Å. It is about twice that obtained in experiments by Mandurah *et al.* [26] for conditions not very different of our conditions. The equilibrium grain boundary segregation coefficient  $k_{seg0}$  is described by an expression analogous to one used in Mandurah *et al.* [26] for arsenic ( $k_{seg0} = k_0 \exp(0.456/KT)$ ).

The parameter  $k_0$  was chosen equal to  $5.2 \times 10^{-9}$ . It means that the effect of segregation for boron in these conditions is approximately 4 times as low as for arsenic [24], [26]. The good adjustment will be carried out if we used the average initial grain size  $L_{g0}$  of the order of 100 Å or less than this value. This last value is approximately 8 times lower than that obtained in experiments by Akhtar *et al.* [27]; through atomic force microscopy (AFM) for polysilicon films obtained by LPCVD at 620°C from silane ( $\text{SiH}_4$ ).

This is justified by the initially amorphous films deposited by LPCVD at lower temperature (465°C) [11]. We assume that the deposited films by LPCVD at 465°C starting from disilane ( $\text{Si}_2\text{H}_6$ ), provides grains of very small sizes with an important density ( $L_g < 100$  Å). These grains are further grouped in the form of very small clusters of silicon-atoms. In each cluster the grains maintain their individual identity [27]. Annealing of the polycrystalline-silicon films at 700, 750, and 800°C diminishes the clusters density and increases the grains size; grain boundaries are eliminated by grains growth through normal recrystallization.

The grain length increase during annealing from the nearly clusters (union of clusters) or starting from the near disordered regions; some grains grow at the expense of neighboring grains. Growth kinetic or recrystallization is normal if the films are undoped. However, if the films are heavily doped, grains growth is greatly influenced and enhanced. This dopant-enhanced grain growth is a strong function of the dopant concentration. Figure 9 shows that little enhanced grain-growth occurs below a boron concentration of  $1 \times 10^{19} \text{ cm}^{-3}$ . However, more important enhancement of the grain-growth appears in heavily doped region. This grain-growth enhancement is limited at very high boron concentrations ( $C_B > C_{sol}$ ) because boron-clusters and boron-precipitates impede grain boundary elimination.

The driving force for grain growth is the reduction in grain boundary energy as grain boundaries are eliminated by grain growth. In consequence, it has been assumed that vacancies with different charge states (which depend on the location of the Fermi level in the band gap) accelerate grain-boundary migration. Since the crystallization is not uniform along the film depth because the doping concentration is not uniform, it's very possible that there will be three regions of different grains sizes after some seconds of annealing. Region of large almost uniform grains, region of medium less uniform grains and region of smaller grains approximately not uniform.

The dopant diffusivity in each region is influenced by the crystallization velocity rate and effects of impurity concentration. As the grains grow faster, the total grain boundary volume decreases and thus the concentration in the grain boundary drops. As mentioned before, grain growth is a strong function of the dopant concentration and so is maximum near the peak region. Probably, the boron clusters and precipitates are quickly surrounded in this region by the silicon atoms and crystallites to construct larger grains (primary and secondary crystallization).

As can be seen from figures 3–8, the nonreduction in the peak from the as-implanted profile is because of  $C_{sol}$  effects and boron transfer towards the grains; boron clusters and boron precipitates are encircled to be transferred inside the crystallites as a result of the considerable grain growth occurring in this region. It can be clearly seen that in the peak region of the profiles ( $C_{Btot} > C_{sol}$ ) much of the boron is transferred in the grains; since grain boundary volume is considerably reduced.  $D_{gb}^{eff}$  and  $D_g^{eff}$  are considerably decreased. Near and below solubility limit  $C_{sol}$ , the activity of boron is more and more significant and the driving force for grain growth is less significant than before.

Therefore, for medium grain size ( $n_i < C_{Btot} < C_{sol}$ ), the grain growth is medium and grain boundary volume is more, so the concentration of boron in the grain boundary is higher; most of the dopant is in the grain boundaries. The profile shoulder (bump) that occurs near the boron solubility limit is because of boron slower transfer from the large grains (peak region) to the grain boundaries, followed by fast diffusion along these grain boundaries (following region).

This fast diffusion in the grain boundaries gives rise to the fast decrease of the impurity concentration which appears immediately after the profile shouldering. The high-defects concentration inside the grain boundaries due to its elimination accelerate dopant diffusivity. However, in the tail region ( $C_{Btot} < n_i$ ), smaller grain size means a larger grain boundary volume which leads to more trapping-segregation mechanism in the grain boundary; so most of the dopant is in the grain boundaries.

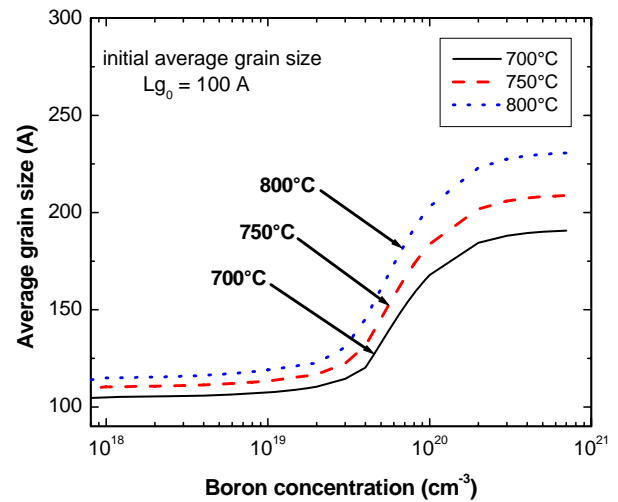


**Figure 9** : Growth of grains as a function of the boron concentration during 1 minute of annealing.

The vacancies concentration effects on boron diffusivity depends principally of  $\beta$ . Its optimal value obtained after profiles adjustment is 0.13 which is in good agreement with that in studies of Mahamdi *et al.* [11] and Giroult *et al.* [28]. The adjustment factor of diffusivity in the grain boundaries given in the theory by the ratio  $D_{poly}/D_{mono}$  is approximately 100 in our simulation. This means that the boron diffusivity in the grain boundaries is about 100 times greater than that in the grains.

This result is consistent with that obtained by Probst *et al.* [18]. The number of self-interstitials to be trapped in boron clusters,  $m$ , takes the value of  $m = 2$  which lead to the best fitting for all the profiles. This  $m$  value is approximately similar to that obtained by Uematsu for heavily-implanted monocrystalline silicon [6], [9]. In effect, the presence of high self-interstitial concentration causes transient enhanced diffusion (TED) of dopant atoms and their precipitation into clusters at a concentration well below the solubility solid limit. This was observed in rigorous manner in the simulated profiles by the shoulder (bump) of the diffusion profiles that occurs with the boron solubility solid limit. This effect was also discussed in research of Pelaz *et al.* [5], [15] and research of Mahamdi *et al.* [11].

### CONCLUSION

According to the results of this study, grains-growth and high-concentration effects are two very significant parameters for the precise simulation of the diffusion profiles. Owing to polycrystalline structure, the segregated impurities add a number of degrees of freedom to its parameters, which are responsible to influence of various physical and electrical properties of the polysilicon films. We can note that boron transient enhanced diffusion (TED) does not depend only on the trapping and segregation to the grains boundaries, but also on clustering effect to the grains; under the effects of the strong concentrations. Moreover, boron-enhanced grain growth is a strong function of the boron concentration. For all high doses implantation cases the trapping-segregation mechanism between grains and grain boundaries as well as growth of grains are the major effects during thermal annealing process.

### REFERENCES

- [1] B. Yu, D. H. Ju, W. C. Lee, N. Kepler, T. J. King and C. Hu, "Gate engineering for deep-submicron CMOS transistors," *IEEE, Trans. Electron Devices*, Vol. 45, (1998), pp. 1253-1262.
- [2] A. J. Walker, S. B. Hermer, T. Kumar and En-H. Chen, "On the conduction mechanism in polycrystalline silicon thin-film transistors," *IEEE, Trans. Electron Devices*, Vol. 51, No. 11, (2004), pp. 1856-1866.
- [3] J. R. Pfister, F. K. Baker, T. C. Mele, H. H. Tseng, P. J. Tobin, J. D. Hayden, J. W. Miller, C. D. Gunderson and L. C. Parillo, "The effects of boron penetration on P<sup>+</sup> polysilicon gated PMOS devices," *IEEE Trans. Electron Devices*, Vol. 37, No. 8, (1990), pp. 1842-1847.
- [4] T. Aoyama, K. Suzuki, H. Tashiro, Y. Tada, H. Arimoto, and K. Horiuchi, "Flatband voltage shift in PMOS devices caused by carrier activation in p<sup>+</sup> polycrystalline silicon and by boron penetration," *IEEE, Trans. Electron Devices*, Vol. 49, (2002), pp. 473-479.
- [5] L. Pelaz, V. C. Venezia, H. J. Gossmann, G. H. Gilmer, A. T. Fiory, and C. S. Rafferty, "Activation and deactivation of implanted B in Si," *Appl. Phys., Lett.*, Vol. 75, No. 5, (1999), pp. 662-664.
- [6] Masashi Uematsu, "Simulation of high-concentration boron diffusion in silicon during post-implantation annealing," *Jpn. J. Appl. Phys.*, Vol. 38, (1999), pp. 3433-3439.
- [7] M. Jaraiz, G. H. Gilmer and J. M. Poate, "Atomistic calculations of ion implantation in Si: point defect and transient enhanced diffusion phenomena," *Appl. Phys., Lett.*, Vol. 68, No. 3, (1996), pp. 409-411.
- [8] H. Schaber, R. V. Criegern and I. Weitzel, "Analysis of polycrystalline silicon diffusion sources by secondary ion mass spectrometry," *J. Appl. Phys.*, Vol. 58, No. 11, (1985), pp. 4036-4042.
- [9] Masashi Uematsu, "Simulation of clustering and transient enhanced diffusion of boron in silicon," *J. Appl. Phys.*, Vol. 84, No. 9 (1998), pp. 4781-4787.
- [10] J. Marcon, L. Ihaddadene-Le Coq, K. Masmoudi and K. Ketata, "An investigation on the modeling of boron-enhanced diffusion of ultralow energy implanted boron in silicon," *Materials Science and Engineering, B*, 124-125 (2005), pp. 415-418.
- [11] R. Mahamdi, F. Mansour, E. Scheid, P.T. Boyer and L. Jalabert, "Boron diffusion and activation during heat treatment in heavily doped polysilicon thin films for P<sup>+</sup> Metal-Oxide-Semiconductor transistors gates," *Jpn. J. Appl. Phys.*, Vol. 40, (2001), pp. 6723-6727.
- [12] R. W. Cahn, P. Haasen, and E. J. Kramer, "Materials Science and Technology: Electronic structure and properties of semiconductors," Ed. Weinheim New York: Basel-Chambridge, Vol. 4, (April 1991), pp. 254-275.
- [13] S. Solmi, F. Baruffaldi and R. Canteri, "Diffusion of boron in silicon during post-implantation annealing," *J. Appl. Phys.*, Vol. 69, No. 4, (1991), pp. 2135-2142.
- [14] S. Batra, M. Manning, C. Dennison, A. Sultan, S. Bhattacharya, K. Park, S. Banerjee, M. Lobo, G. Lux, C. Kirschbaum, J. Noberg, T. Smith and B. Mulvaney, "Discontinuity of B-diffusion profiles at the interface of polycrystalline Si and single crystal Si," *J. Appl. Phys.*, Vol. 73, No. 8, (1993), pp. 3800-3804.
- [15] L. Pelaz, G. H. Gilmer, H. J. Gossmann, C. S. Rafferty, M. Jaraiz and J. Barbella, "B cluster formation and dissolution in Si: A scenario based on atomic modeling," *Appl. Phys., Lett.*, Vol. 74, (1999), pp. 3657-3660.
- [16] H. Puchner and S. Selberherr, "An advanced model for dopant diffusion in polysilicon," *IEEE, Trans. Electron Devices*, Vol. 42, No 10, (1995), pp. 1750-1754.
- [17] A. D. Sadovnikov, "One-dimensional modeling of high concentration boron diffusion in polysilicon-silicon structures," *Solid-State Electronics*, Vol. 34, No. 9, (1991), pp. 969-975.
- [18] V. Probst, H. J. Bohm, H. Schaber, H. Oppoler and I. Weitzel, "Analysis of polysilicon diffusion sources," *J. Electrochem Soc.*, Vol. 135, No. 3, (1988), pp. 671-676.
- [19] R. B. Fair, "Concentration profiles of diffused dopants in silicon," *Impurity Doping Processes in Silicon*, F. F. Y. Wang, Ed. New York: North Holland, (1981), pp. 315-442.

- [20] J. Y. W. Seto, "The electrical properties of polycrystalline silicon films," *J. Appl. Phys.*, Vol. 46, No. 12, (1975), pp. 5247-5254.
- [21] G. Baccarani, B. Ricco and G. Spadini, "Transport properties polycrystalline silicon films," *J. Appl. Phys.*, Vol. 49, (1978), pp. 5565-5570.
- [22] S. K. Jones and C. Hill, "Modeling dopant diffusion in polysilicon," *Simulation of Semiconductor Devices and processes*, Vol. 3, (1988), pp. 441-449.
- [23] H.-J. Kim and C.V. Thompson, "Kinetic modeling of grain growth in polycrystalline silicon films doped with phosphorus or boron," *J. Electrochem. Soc.*, Vol. 135, (1988), pp. 2312-2316.
- [24] M. M. Mandurah, K. C. Saraswat, C. R. Helms and T. I. Kamins, "Dopant segregation in polycrystalline silicon," *J. Appl. Phys.*, Vol. 51, No. 11, (1980), pp. 5755-5763.
- [25] B. Swaminathan, E. Demoulin, T. W. Sigmon, R. W. Dutton and R. Rif, "Segregation of arsenic to the grain boundaries in polycrystalline silicon," *J. Electrochem Soc.*, Vol. 127, No. 10, (1988), pp. 2227-2229.
- [26] M. M. Mandurah, K. C. Saraswat, C. R. Helms and T. I. Kamins, "A model for conduction in polycrystalline silicon – Part II: comparison of theory and experiment," *IEEE, Trans. Electron Devices*, Vol. ED-28, No. 10, (1981), pp. 1171-1176.
- [27] J. Akhtar, S. K. Lamichhane, P. Sen, "Thermal-induced normal grain growth mechanism in LPCV polysilicon film," *Materials Science in Semiconductor Processing*, Vol. 8, (2005), pp. 476-482.
- [28] G. Giroult, A. Nouailhat and M. Gauneau, "Study of  $\text{Wsi}_2$  / polycrystalline silicon / monocrystalline silicon structure," *Appl. Phys.*, Vol. 67, (1990), pp. 515-523.